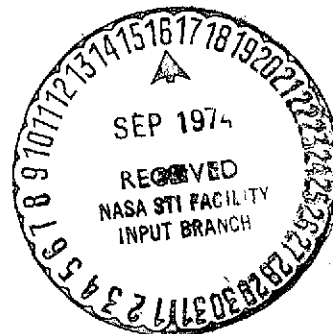


"MARS-3": PRESSURES AND ALTITUDES
BASED ON THE RESULTS OF CO₂ ALTIMETRY

L. V. Ksanfomaliti, V. I. Moroz,
B. S. Kunashev, and V. S. Zhegulev

| | | |
|---|-----------------------|-----------|
| (NASA-TT-F-15910) | MARS-3: PRESSURES AND | N74-32270 |
| ALTITUDES BASED ON THE RESULTS OF CO ₂ | | |
| ALTIMETRY (Kanner (Leo) Associates) | 39 p | |
| HC \$5.00 | CSCL 03B | Unclass |
| | G3/30 | 47735 |

Translation of "'Mars-3': Davleniya i vyosoty po rezul'tatam
CO₂-al'timetrii," Institute of Space Research,
USSR Academy of Sciences, Moscow,
Report Pr-183, 1974, 41 pp.



STANDARD TITLE PAGE

| | | | | | |
|--|--|-----------------------------|--|--|--|
| 1. Report No. NASA TT F-15910 | | 2. Government Accession No. | | 3. Recipient's Catalog No. | |
| 4. Title and Subtitle "MARS-3": PRESSURES AND ALTITUDES BASED ON THE RESULTS OF CO ₂ ALTIMETRY | | | | 5. Report Date September 1974 | |
| | | | | 6. Performing Organization Code | |
| 7. Author(s) L. V. Ksanfomaliti, V. I. Moroz, B. S. Kunashev, and V. S. Zhegulev, Institute of Space Research, USSR Academy of Sciences, Moscow | | | | 8. Performing Organization Report No. | |
| | | | | 10. Work Unit No. | |
| 9. Performing Organization Name and Address Leo Kanner Associates Redwood City, California 94063 | | | | 11. Contract or Grant No. NASw-2481 | |
| | | | | 13. Type of Report and Period Covered Translation | |
| 12. Sponsoring Agency Name and Address National Aeronautics and Space Adminis- tration, Washington, D.C. 20546 | | | | 14. Sponsoring Agency Code | |
| | | | | | |
| 15. Supplementary Notes Translation of "Mars-3": Davleniya i vysoty po rezul'tatam CO ₂ -al'timetrii," Institute of Space Research, Academy of Sciences USSR, Moscow, Report Pr-183, 1974, 41 pp. | | | | | |
| 16. Abstract Variations in the 2-micron CO ₂ band intensities were measured from the "Mars-3" orbiter, giving relative pressures and al- titudes. The overall range of altitude changes was close to 8 km. There is some correlation between albedo and altitude, on a scale of hundreds of kilometers: dark regions are higher (statistically) than neighboring bright ones. The upper boundary of dust clouds during the storm was 10-15 km in the equatorial region of the planet. | | | | | |
| 17. Key Words (Selected by Author(s)) | | | 18. Distribution Statement Unclassified-Unlimited | | |
| 19. Security Classif. (of this report) Unclassified | 20. Security Classif. (of this page) Unclassified | | 21. No. of Pages 37 | 22. Price | |

"MARS-3": PRESSURES AND ALTITUDES
BASED ON THE RESULTS OF CO₂ ALTIMETRY

L. V. Ksanfomaliti, V. I. Moroz,
B. S. Kunashev, and V. S. Zhegulev

Institute of Space Research,
USSR Academy of Sciences, Moscow

1. Introduction

/3*

It was considered for a long time that the surface of Mars was smoother than those of the moon and the Earth. It has become clear in recent years that this classical point of view is far from true. Many craters, tremendous volcanic cones and gigantic fractures have been found on Mars. The shape of the planet differs considerably from equilibrium. The difference in altitude between the highest and lowest regions reaches 20 km.

Quantitative information on the macrorelief of Mars was first obtained in 1967, by means of ground pulse radar [1]. It has been significantly supplemented since that time. Five methods have been used:

1. Pulse radar [2-5];
2. Determination of the local radius in a radio occultation experiment [6,7];
3. Measurement of intensity of absorption in the CO₂ infrared bands, with high spatial resolution (from ground observations [8-10] and measurements from spacecraft [11-13]);
4. Determination of atmospheric pressure in a radio occultation experiment [6,14];
5. Determination of the optical thickness of the atmosphere

* Numbers in the margin indicate pagination in the foreign text.

in the near ultraviolet region, with high spatial resolution [15-17].

The first two methods give the distance from the center of /4 mass, and the remaining three, the altitude above a certain equipotential surface. Method (1) is the most accurate; in individual cases, the distance error amounts to a few tens of meters; however, its use is limited to the zone close to the equator, from -23° to $+23^\circ$, with only a few narrow bands having been examined in this zone up to now. Methods ((2) and (4) permit data to be obtained only for a selected number of points, by the number of occultations observed. It was over 100 in the case of Mariner-9; however, this is too few for an isohypse map. Finally, Methods (3) and (5) are the least accurate, their error being on the order of ± 1 km, but then, they permit study of extensive sections of the planet. At least four maps have been compiled by these methods, giving surface isohypses, with averaging from 5 to 10° in a zone from approximately -60° to $+20^\circ$ [8,10,12,17]. Two of them, compiled from the results of IR and UV spectroscopy on Mariner-9 [13, 17], demonstrate better mutual agreement, and they obviously merit the greatest trust.

A photometer, specially intended for determination of the pressure and altitude profiles on the surface of the planet from the CO_2 band intensity, was installed on the Soviet "Mars-2" and "Mars-3" orbital spacecraft. The results obtained on "Mars-3" have been published in part previously [12,18,19]; a more complete presentation of them and some analyses are given here.

2. Method, Instruments, Calibration

The concept of the method is as follows. In formation of molecular bands in the reflected radiation spectrum, their intensity depends on the total amount of absorbing matter in the visual pathway, i.e., in the sun-point observed-instrument path. This quantity in vertical incidence and reflection is proportional /5

to the total pressure and, in the general case, it also is a function of the angles of incidence and reflection. Under otherwise equal conditions, the higher region will be characterized by less intense absorption bands and vice versa. Conversion of intensity into pressure is accomplished in a quite direct manner, if scattering in the atmosphere can be disregarded.

In the normal state of the Martian atmosphere (excepting periods of dust storms), its optical scattering thickness is negligibly small in the $\lambda > 1\mu\text{m}$ region of the spectrum. At the same time, carbon dioxide, of which the atmosphere mainly consists, has quite strong absorption bands here, which are convenient for determination of relative altitudes. In observations from Earth, bands of moderate intensity have been used (about 1.05 and $1.6\mu\text{m}$ [8-10]), since interference on the part of terrestrial CO_2 has less effect in this case. In observations from orbit, it is more advantageous to use the stronger group of bands at around $2\mu\text{m}$. The first determinations of relative pressures and altitudes, using the $2\mu\text{m}$ CO_2 band, were carried out on the American spacecraft Mariner-6 and Mariner-7 [11]. On Mars-3, the spectral region around $2\mu\text{m}$ also was used for CO_2 altimetry (as we will call this method subsequently, for brevity). This region (see Fig. 1) contains three strong bands (04°I , 12°I and 20°I) and many weak ones, hot and isotopic ones.

The strong bands consist of saturated rotational lines. The equivalent width of an isolated, saturated rotational line equals

$$W = 2.5 (u s P_e \Delta\nu_0)^{1/2} \left(\frac{293}{T_e} \right)^{1/4} \quad (1)$$

where u is the amount of gas absorbed in $\text{cm}\cdot\text{atm}$, s is the integral coefficient of absorption in the line at $1\text{ cm}\cdot\text{atm}$, P_e is the effective pressure in atm (mean suspended amount of CO_2 in the visual path; in an exponential atmosphere, it equals half the pressure at the surface P_0 ; see [20]), $\Delta\nu_0$ is the Lorentz width of the line under normal conditions (pressure 1 atm and temperature 293°K), and T_e is the effective temperature of the atmosphere.

If it is assumed that the relative CO_2 content is 100 percent,

$$u = P_0 H_0 M \quad (2)$$

where H_0 is the scale height at $T = 273^\circ\text{K}$, M is the air mass, equal approximately to a plane stratified atmosphere

$$M = \frac{1}{\mu_1} + \frac{1}{\mu_2} \quad , \quad (3)$$

where μ_1 is the cosine of the angle of incidence and μ_2 is the cosine of the angle of reflection.

Using (2), (1) can be presented in the form

$$W = P_0 (2 H_0 M S \Delta \nu_0)^{1/2} \left(\frac{293}{T_0} \right)^{1/4} \quad (4)$$

The equivalent band width

$$W_b = f(T_0) \cdot \bar{W} \quad (5)$$

where \bar{W} is the equivalent width of the strongest line in the band. Coefficient $f(T)$ plays the part of effective number of lines in the band.

In a similar manner, for a laboratory cuvette of length l , filled with CO_2 at pressure P_l and temperature T_l , we have

$$W_l = 2 P_l (l S \Delta \nu_0)^{1/2} \left(\frac{293}{T_l} \right)^{3/4} \left(\frac{273}{293} \right)^{1/2} \quad (6)$$

and

$$W_{bl} = f(T_l) \cdot W_l \quad (7)$$

If identical equivalent band widths are obtained in the spectrum of Mars and in the laboratory, we have

$$\rho_0 = \rho_0 \left(\frac{2\ell}{4M} \right)^{1/2} \left(\frac{T_0}{T_0} \right)^{1/4} \left(\frac{293}{T_0} \right)^{1/4} \left(\frac{293}{293} \right)^{1/2} \quad (8)$$

where

$$c = \frac{f(T_0)}{f(T_0)} \cdot \left(\frac{S_0}{S} \right)^{1/2} \quad (9)$$

The quantities $f(T)$, S and C depend on temperature. Moreover, ⁷ they also are functions of pressure, although very slightly.

For determination of the relative altitudes, only the relative pressure in various sections of the planet are essential. Altitude difference ΔZ_{12} between sections 1 and 2, with pressures P_1 and P_2 , respectively, equal

$$\Delta Z_{12} = H \ln \frac{P_1}{P_2} = H \ln \left[\frac{P_{01}}{P_{02}} \left(\frac{M_2}{M_1} \right)^{1/2} \left(\frac{T_{e1}}{T_{e2}} \right)^{1/4} \right] \quad (10)$$

where P_{01} and P_{02} are the laboratory pressures corresponding to the same equivalent widths as in the Mars spectrum and T_{e1} and T_{e2} are the atmospheric temperatures above sections 1 and 2.

For determination of the CO_2 band intensity at various points on the planet, a photometer with interference filters was used in the Mars-3 orbital spacecraft. Its optical system is presented in Fig. 2. Cassegrain lenses R_1 and R_2 (diameter 40 mm, aperture ratio 1:15) focuses the radiation from the planet on two sulphur-lead photoresistors P_1 and P_2 . The beam is divided by means of rotating mirror modulator M . One of the photoresistors P_1 records radiation only in a continuous spectrum, and it serves as a sensor of the automatic gain regulation system, eliminating dependence of the instrument output signal on brightness of the planet over a wide range. Interference filter F_1 , at wavelength $2.2\mu m$, is installed in front of this photoresistor. Filters F_2-F_6 , four of which are in the CO_2 band region and the fifth in a continuous spectrum, are engaged sequentially in front of the second photoresistor. The ratio of the readings with filters in the CO_2 band to the readings with the $2.2\mu m$ filter are a measure of the equivalent

width of the $2.05\mu\text{m}$ band and the laboratory calibrations connected with it. The width of the filters is about 200 Å at the 0.5 level. Transmission of the filters as a function of wavelength is given in Fig. 1.

The field of view of the instrument is 0.01 radians (15 km at a distance of 1500 km); however, the measurements are averaged over a larger area, since the actual processing procedure consisted of averaging the readings of four successive turns, taking up 12 sec, in the course of which the spacecraft travels about 50 km. These groups are recorded at 36 sec intervals, which corresponds to approximately 150 km next to the pericenter.

In processing, there was a ratio of the readings with each filter to the reading with the $2.2\mu\text{m}$ filter: 2/6, 3/6, 4/6 and 5/6. A correlation curve was then plotted between the 4/6 (or 2/6; filters 4 and 2 distinguished the region of the spectrum next to the center of the $2.05\mu\text{m}$ and $2.01\mu\text{m}$ bands, respectively) and the remaining three filters. All readings were converted to the 4/6 (or 2/6) system by this correlation curve, and they were the average of four values in one rotation of the disk. The average values of four turns were then determined and the root mean error of this latter value was calculated. The equivalent width was connected to the reading ratio by a dependence of the type

$$W = a(b - x),$$

where x is the reading ratio, corrected to the 4/6 system, $x \rightarrow b$ as $W \rightarrow 0$. Constants a and b were determined from the laboratory calibrations.

The photometer was rigidly fastened to the spacecraft hull, and its orientation in a constant direction during the measurements usually was provided by the spacecraft sun-star orientation system. Upon approaching the pericenter of the orbit, it was turned on, together with other instruments of the astrophysical set, a few minutes before crossing the limb, by a special optical sensor. The

optical axis usually crossed the planet along a line, which was close to a great circle, and passage from limb to limb took about 30 minutes. In the future, we will call the track of the optical axis on the surface of the planet the measurement course. According to preliminary estimates, the accuracy with which the measurement course is determined is 1-2 degrees in areographic coordinates.

The period of rotation of Mars-3 is about 12 days. Seven /9 measurement courses accomplished by this spacecraft are shown in Fig. 3. The distance at the pericenter to the surface of Mars changes somewhat as the orbit evolves, and it was approximately from 1000 to 1500 km during this period. The first three passages, 15 December 1971, 27 December 1971 and 9 January 1972, occurred during the time of a dust storm and during the period it died away, and the remaining, after the end of the dust storm. In December, January and February, the measurement courses corresponding to successive dates of passage of the periares shifted relative to one another by approximately 90° in longitude. As a result, considerable sections of the 3 February 1972, 16 February 1972 and 28 February 1972 courses pass close to the 15 December 1971, 27 December 1971 and 9 January 1972 courses, and we have measurements for the same regions of Mars, obtained during the time of the storm (more precisely, during its last stages) and after the storm. The 12 March 1972 course, for a number of reasons, still has not been successfully tied to the surface with a sufficient degree of reliability, and its position, designated in Fig. 3, should be considered to be approximate.

The measurements were essentially of a complex nature. Simultaneously with the CO_2 altimetry, measurements of the brightness of the reflected solar radiation, surface temperature and H_2O content in the atmosphere were carried out along the same courses [12,18,19,21-24].

3. Measurement Results

The equivalent widths of the $2.05\mu\text{m}$ CO_2 band, measured along six measurement courses of Mars-3 are presented in Figs. 4-9. They are given as functions of Moscow time, but the areographic coordinates, tying the measurements to the surface, also are plotted along the abscissa. The root mean air mass is given in this same series of graphs. In the first approximation, the equivalent width is directly proportional to the pressure at the surface and to the /10 root mean air mass.

At constant pressure, change in equivalent width along a course will be determined by the air mass. The latter increases sharply close to the beginning and end of a course, and the behavior of the equivalent widths can serve here, to a certain extent, as a control of the correctness of the results. In particular, if the atmosphere is saturated with dust, as occurred during the dust storm period, the pattern of change in equivalent width close to the edge will be completely different. If the absorption band is formed in clouds, its equivalent width does not increase, but it decreases with increase in air mass. This is observed in the 27 December course and in the northern (located near the equator) sections of the 15 December and 9 January courses.

Therefore, to produce any conclusions as to the relief, with a sufficient degree of reliability, principally the three February courses have to be used. The January course can be used in part (approximately up to the intersection with the equator). The two December courses can then give information on cloud height.

Altitudes, calculated from the equivalent widths measured along the Mars-3 course, are presented in Figs. 10-15. They are given in dotted lines, in those cases when the atmosphere above the course was dusty, and the measurement results may be spoiled by scattering in the atmosphere. The distribution of brightness of the reflected solar radiation along the courses, measured at the $1.4\mu\text{m}$ wavelength (H_2O photometer, Mars-3, see [21-23]), also

are shown in these figures. The presence of photometric measurements on the same course permits investigation of the question of a possible correlation between surface albedo and altitude.

The scale height was assumed to be constant and equal to 11 10 km. The 6.1 mb pressure level, corresponding to the triple-point of water, was selected as the initial level for altitude readings. This choice of the zero altitude level for Mars was proposed by Bart [16], and it recently has become generally accepted.

For comparison, data on altitudes obtained by ground radar measurements (in places where the radar profile intersects our courses), as well as altitudes determined in the Mariner-9 radio occultation experiment (in cases, when the occultation points were located sufficiently close or sufficiently confident interpretations could be made), are plotted on the same graphs.

In addition, our courses were plotted on hypsometric charts, produced from ground observations [10], from the ultraviolet optical thickness of the atmosphere (Mariner-9, [17]) and from measurements in the $15\mu\text{m}$ CO_2 band (Mariner-9, [13]). The profiles obtained as a result of this superposition also are given in Figs. 10-15. They all are significantly smoother than our measured profiles. The reason for the difference most likely is the circumstance that hypsometric charts were compiled with much averaging ($5-10^\circ$).

The radio occultation altitudes used for comparison were determined from the value of the pressure at the occultation point, i.e., they can be compared directly with our results. The matter is more complicated with the radar profiles. In the original publications, they are not tied to a definite pressure level and, moreover, such a zero point may differ on different parts of the planet, because of deviations from spherical of the shape of the equipotential surface. The radar profiles which we used are presented in Fig. 16. The altitude at longitude 30° was provisionally adopted as the zero level. Asphericity of the equipotential surface was not taken into account.

We initially consider the information obtained, under conditions of a dust-free atmosphere. We begin with the 9 January course (Fig. 10). It travels initially in the southern latitudes, and it then turns to the northeast. The altitudes experience considerable fluctuation, but, on the average, they decrease along the course. The terrestrial and Mariner profiles confirm this general tendency. An altitude of 6-7 km is observed in Mare Australe, and it fluctuates between 0 and 3 km in Mare Erythraeum and Margaritifer Sinus. The lowest regions on the course are the bright Argyre and dark Margaritifer Sinus regions. A definite correspondence between altitude and brightness is noticeable in a number of cases. The dark region between Mare Australe and Argyre is, for example, higher than its surroundings. At the northern end of the course, our profile goes much higher than all the remaining data; the measurements evidently are spoiled by the dust cloud residues. here.

The 3 February course (Fig. 11) is the shortest one, and the measurements were interrupted at the eighth minute, for technical reasons. In the existing section, passing through Hersonesus, Eridanis and the southern edge of Mare Cimmerium, the altitudes are quite high, 3-4 km.

The 16 February course intersects interesting regions (Fig. 12): the lowland region of Hellas, the severely broken and quite high (up to 4 km) Syrtis Major, the northern hemisphere with its characteristic general subsidence. It is interesting that there are systematic differences in altitude here, between all measurements from orbital spacecraft, on the one hand, and ground (radar and spectroscopic), on the other. The first give 3-4 km lower altitudes than the second, in the zone of the equatorial seas (Syrtis Major).

On the other hand, all data on the 28 February course (Fig. 13) (with the exception of the 1967 radar points) generally agree satisfactorily, although there are divergences on the order of 1 km. The altitudes increase at the southern and northern ends of the course

(to approximately 4 km), and they decrease to zero and even negative values in the equatorial region. /13

The root mean error in determination of altitudes, calculated by the method described above, fluctuates about the value of ± 1 km. Smaller errors correspond to lower heights on the average.

4. Which Are Higher: Dark or Light Regions?

The question of relative altitudes of the dark and light regions is the subject of long discussions. The point of view initially propagated was that the seas are lower than the continents, since they are warmer. However, this argument is highly unconvincing, since the differences in temperature can be entirely explained by differences in albedo, and they give no information on altitude. Sagan, Pollack and Goldstein [25], on the basis of analysis of radar reflection coefficients, reached the opposite conclusion: the seas, as a rule, are higher than the continents. Direct information on the altitudes on Mars, which began to come in approximately seven years later, generally did not confirm either of these hypotheses; it showed that the seas can be high and low regions. The Mariner photos disclosed that the seas and continents frequently do not differ in topographic or geologic structure.

It should be noted, however, that a detailed comparison of the topography and photometry was impossible until recently, for a reason which was very convincing at first glance: there were no photometric data of the necessary accuracy. Modern radar profiles of Mars cannot be compared with the photometric ones, simply because there are no photometric measurements of comparable accuracy and spatial resolution. Mars-3 in essence first carried out simultaneous determinations of altitude and precise photometry on identical sections of the planet.

A qualitative comparison of the altitude profiles and the photometric profiles leads to the following conclusions: at large scale (on the order of thousands of kilometers), the dark regions /14

may be high or low, with approximately equal probabilities, and the same can be said of the light ones. However on scales of hundreds of kilometers, the darker regions frequently turn out to be higher than nearby light ones.

In Figs. 17 and 18, altitudes are plotted on the abscissa and the relative brightness factors on the ordinate

$$R = \frac{B\pi}{\mu_1} \text{const.}$$

where B is the brightness, μ_1 is the cosine of the angle of incidence; its values for the Mars-3 courses are given in work [21]. Points in the equatorial sea regions and the high-latitude continental ones are marked separately. The statistical dependence of the relative brightness factor on altitude, for the 16 and 28 February sessions, are presented in Table 1. This dependence quantitatively characterizes the tendency of the darker regions to be higher. Average altitudes along each course are given there. The average altitude of two sessions is 1.2 km, and the pressure, 5.3 mb. However, it should be noted that our pressure system is not absolute. It depends on a choice of coefficient c in formula (8). The value $c = 0.56$, which we used, was selected, so that equivalent width of the $2.05\mu\text{m}$ band, obtained from ground spectroscopic observations of the entire of the entire disk of Mars (22.5 cm^{-1} , according to [20]), gave an average pressure over the planet of 6 mb.

Table 1

| Course | Average altitude, km | Dependence of Relative Brightness Factor R on Altitude Z |
|------------------------|----------------------|--|
| 16.2.72/ ^x | 0.82 | $R = 0.259 (\pm 0.003) - 0.014 (\pm 0.004)Z$ |
| 28.2.72/ ^{xx} | 1.63 | $R = 0.310 (\pm 0.003) - 0.013 (\pm 0.007)Z$ |

/^x between points $\varphi = -29^\circ$, $\lambda = 301^\circ$ and $\varphi = +20^\circ$, $\lambda = 285^\circ$.

/^{xx} beginning at point $\varphi = -36^\circ$, $\lambda = 39^\circ$ to the end of the course.

5. How High Does the Dust Rise During a Dust Storm?

The results of altitude determination on the 15 and 27 December courses, when the dust storm still had not ended, are presented in Figs. 14 and 15. Basically, the altitude estimates for these dates turned out to be significantly higher than the measurements of other authors give. Of course, this is explained by the fact that the solar radiation is not scattered by the surface, but by the dust clouds. The difference between the altitudes measured in this case and in other experiments determines a certain effective altitude at which reflection takes place. This effective altitude will equal the height of the upper boundaries of the clouds, if they are sufficiently dense and if multiple scattering can be disregarded. The effective cloud height in the equatorial regions reaches 10 km on the 27 December course.

However, a decrease in equivalent width close to the terminator in the 15 and 27 December sessions indicates a large role for multiple scattering. We are attempting to estimate this effect on the estimate of the position of the upper boundaries of the clouds. In reflections from clouds, a part of the radiation path passes through the atmosphere above the clouds, relatively free of aerosols, and another part within the clouds. We will consider the simplest model, in which the cloud layer is assumed to be uniform in optical properties, bounded from above by a plane surface and semi-infinite. Fig. 19 illustrates the geometry of propagation of radiation in such a medium. If absorption in the purely gaseous atmosphere beneath the clouds is disregarded, the equivalent width of the isolated saturated line can be expressed by the parameters of the scattering medium and pressure (again we assume $100\% \text{ CO}_2$), 16 in the following manner:

$$W = \rho' \left(\frac{\pi^2 a f^2}{2G} S_4 v_0 \right)^{1/2} \left(\frac{293}{T} \right)^{1/4} \left(\frac{293}{P} \right)^{1/2}, \quad (11)$$

where a is the single scattering albedo, recalculated by means of the similarity relationship to a spherical scattering indicatrix,

σ is the bulk scattering coefficient, and f and η_0 are auxiliary functions of albedo and the angles. Formula (11) is a somewhat transformed expression for the equivalent line width in a semi-infinite atmosphere, with an isotropic scattering indicatrix, obtained by Belton [26]. Values of f and η_0 are tabulated in this same work. P' is the effective pressure inside the cloud layer,

$$P' = b \cdot P_c \quad (12)$$

where P_c is the pressure at the upper boundary of the cloud layer, and $b > 1$.

If the line is formed in the atmosphere above the clouds (which is possible at sufficiently high values of σ and at $a < 1$), its equivalent width is determined by formula (1), at $P_e = 1/2 P_c$. If absorption in the cloud layer and above it are comparable in magnitude, a

$$W = P_c (S \Delta \nu_0)^{1/2} \left(\frac{293}{T} \right)^{1/4} \left[2HM + \frac{\pi a b f^2 \eta_0}{2\sigma} \cdot \frac{273}{293} \right]^{1/2} \quad (13)$$

This expression, derived for a semi-infinite scattering medium, can be used in a somewhat rough approximation, in the case of finite optical thickness. Then,

$$\sigma = \frac{Z_0}{Z_0'} \quad (14)$$

where Z_0 is the geometric thickness of the scattering layer. We will assume that the lower boundary of the dust layer coincides with the surface and that Z_0 is the altitude of its upper boundary. We have from (13) and (14)

$$W = W_0 e^{-\frac{Z_0}{H}} \left(1 + \frac{\pi a b \eta_0 f^2}{4 Z_0 M} \cdot \frac{Z_0}{H} \cdot \frac{273}{293} \right)^{1/2} \quad (15)$$

where W_0 is the equivalent line width in a purely gaseous atmosphere. The quantities in parentheses are a correction, due to multiple scattering. We assume $\tau_0 = 1.5$, according to [21], $a = 0.98$, $\eta_0 = 8$, $f^2 = 0.4$, $M = 3$. At $Z = H$ and $b = 2$, this correction increases W by 45%, which corresponds to a 4 km change in altitude. In this manner, taking multiple scattering into consideration can increase the height of the upper boundary of the dust clouds by a factor of approximately 1.5.

Close estimates of the cloud layer altitude, averaged over the disk of the planet, were obtained during the dust storm, as a result of ground measurements of equivalent width of the CO_2 band; true, it was at somewhat earlier stages of it [27,28].

The temperature profile of the atmosphere during the dust storm period, found from Mariner-9 radio occultation measurements, independently indicates the great altitude of the clouds, absorbing solar radiation, and increasing heat fluxes into the atmosphere [6].

6. Conclusions

The principal results of the work can be formulated in the following manner:

1. The altitude difference between the highest and lowest regions on the Mars-3 measurement courses reaches 8 km;
2. There is a correlation between the albedo and altitude, at scales on the order of several hundred kilometers: dark regions, on the average, are higher than light ones located in the vicinity;
3. The upper boundary of the clouds during the dust storm period reached 10-15 km in individual regions.

In conclusion, the authors must thank A. M. Kasatkin, M. Kh. Akhmedeyev, V. G. Budkevich, V. D. Davydov, Z. V. Ivanova, E. N. Luchnikova, Yu. A. Malyugin, L. F. Obukhova, G. N. Petrov, N. V. Temnaya, G. V. Tomasheva, K. A. Tsoy, V. B. Yafayeva and the rest

of the people who cooperated in performing this work at various stages of it.

REFERENCES

1. Pettengill, G. H., C. C. Counselman, L. P. Rainville, and I. I. Shapiro, Astron. J. 74, 461 (1969).
2. Rogers, A. E. E., M. E. Ash, C. C. Counselman, I. I. Shapiro, and G. H. Pettengill, Radio Sci. 5, 465 (1970).
3. Goldstein, R. M., W. Melbourne, G. A. Morris, G. S. Downes, and D. A. O'Handley, Radio Sci. 5, 475 (1970).
4. Pettengill, G. H., I. I. Shapiro, and A. E. E. Rogers, Icarus 18, 22 (1973).
5. Downs, G. S., R. M. Goldstein, R. R. Green, G. A. Morris, and P. E. Reichley, Icarus 18, 8 (1973).
6. Kliore, A. J., D. L. Caini, G. Fjeldbo, B. L. Seidel, M. J. Sykes, and S. I. Rasool, Icarus 17, 484 (1972).
7. Cain, D. L., A. J. Kliore, B. L. Seidel, and M. J. Sykes, Icarus 17, 517 (1972).
8. Belton, M. J. S., and D. M. Hunten, Icarus 15, 204 (1971).
9. Moroz, V. I., N. A. Parfent'ev, D. P. Kryukshenk, L. V. Gromova, Astron. zh. 48, 790 (1971).
10. Parkinson, W. D., and D. M. Hunten, Icarus 18, 29 (1973).
11. Herr, K. C., D. Horn, J. M. McAfee, and G. C. Pimentel, Astron. J. 75, 883 (1973).
12. Moroz, V. I., L. V. Ksanfomaliti, A. M. Kasatkin, B. S. Kuna-shev, and K. A. Tsoya, Dokl. AN SSSR 208, 1048 (1973)
13. Hanel, R., B. Conrath, W. Hovis, V. Kunde, P. Lowman, and others, Icarus 17, 423 (1972).
14. Kliore, A. J., G. Fjeldbo, and B. L. Seidel, "Space Research" XI, p. 165, Akademie Verlag, Berlin (1971).
15. Hord, C. W., Icarus 16, 253 (1971).
16. Hord, C. W., C. A. Bart, A. I. Stewart, and A. L. Lane, Icarus 17, 443 (1972).
17. Hord, C. W., K. E. Simmons, and L. K. Lauhlin, "Mariner 9 Mars Orbiter. Ultraviolet spectrometer experiment. Pressure-altitude measurements on Mars," University of Colorado (1973) (preprint).

18. Moroz, V. I. and L. V. Ksanfomality, Icarus 17, 408 (1972).
19. Moroz, V. I. and L. V. Ksanfomality, Vestnik AN SSSR (9), 10 (1972).
20. Moroz, V. I., Fizika planet [Planetary Physics], Nauka Press, Moscow, 1967.
21. Moroz, V. I., A. E. Nadzhip, V. S. Zhegulev, "Mars-3: Fotometricheskiye profili planety v blizhney infrakrasnoy oblasti spektra [Mars-3: Photometric Profiles of the Planet in the Near Infrared Region of the Spectrum], preprint Inst. of Space Res., USSR Acad. of Sciences, 1974.
22. Moroz, V. I., L. V. Ksanfomality, G. N. Krasovskiy and others, Mars-3: infrakrasnyye temperatury i teplovyye svoystva poverkhnosti planety [Mars-3: Infrared Temperatures and Thermal Properties of the Surface of the Planet], preprint, Inst. of Space Res., USSR Acad. of Sciences, 1974.
23. Moroz, V. I. and A. E. Nadzhip, Mars-3: vodyanoy par v atmosfere planety [Mars-3: Water Vapor in the Atmosphere of the Planet], preprint, Inst. of Space Res., USSR Acad. of Sciences, 1974.
24. Ksanfomality, L. V. and V. I. Moroz, Mars-3: fotoelektricheskaya fotometriya s uzkopolosnymi fil'trami v diapazone 3700-7000 A [Mars-3: Photoelectric Photometry with Narrow-Band Filters in the 3700-7000 A Range], preprint, Inst. of Space Res., USSR Acad. of Sciences, 1974.
25. Sagan, C., J. B. Pollack, R. M. Goldstein, Astron. J. 72, 20 (1967).
26. Belton, M. J. S., J. Atm. Sci. 25, 596 (1968).
27. Parkinson, T. D., D. M. Hunten, Science 175, 323 (1972).
28. Moroz, V. I., O. G. Taranova, Astron. tsirk. (697), (1972).

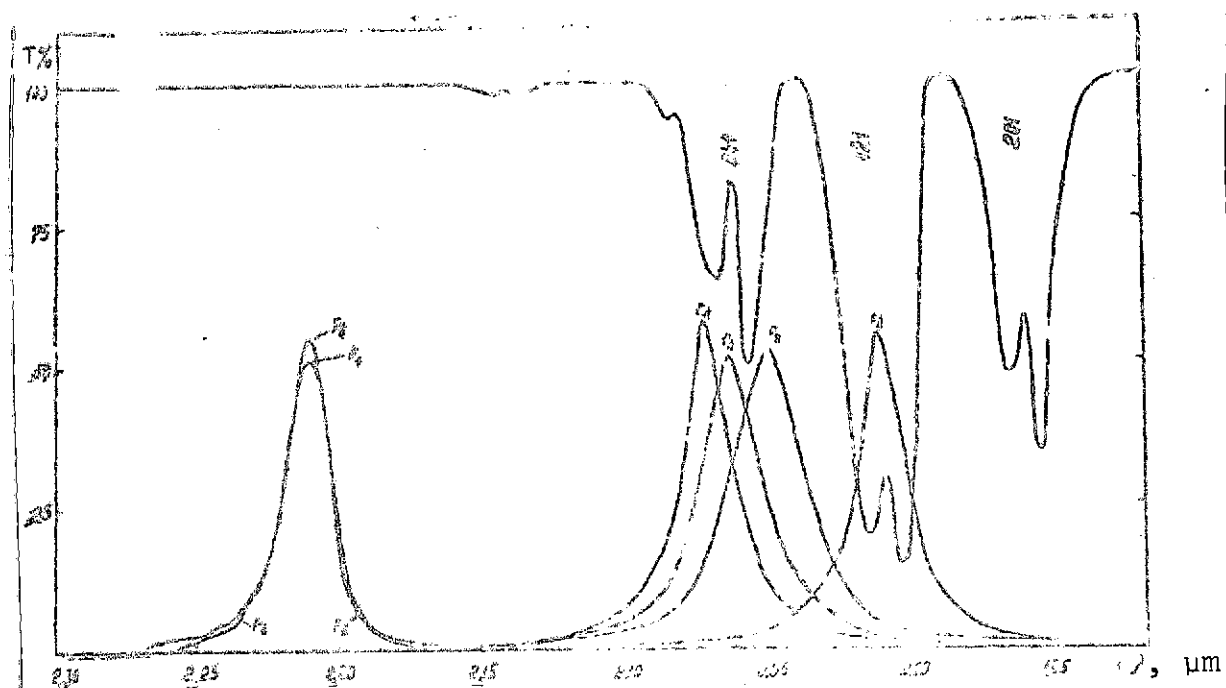


Fig. 1. Carbon dioxide absorption spectrum in 1.92-2.30 μm region. Pressure 1.1 atm, optical path length 2.7 m. Absorption band intensity close to that measured in Mars spectrum. Spectral characteristics of filters used for CO_2 altimetry on Mars-3 are given here.

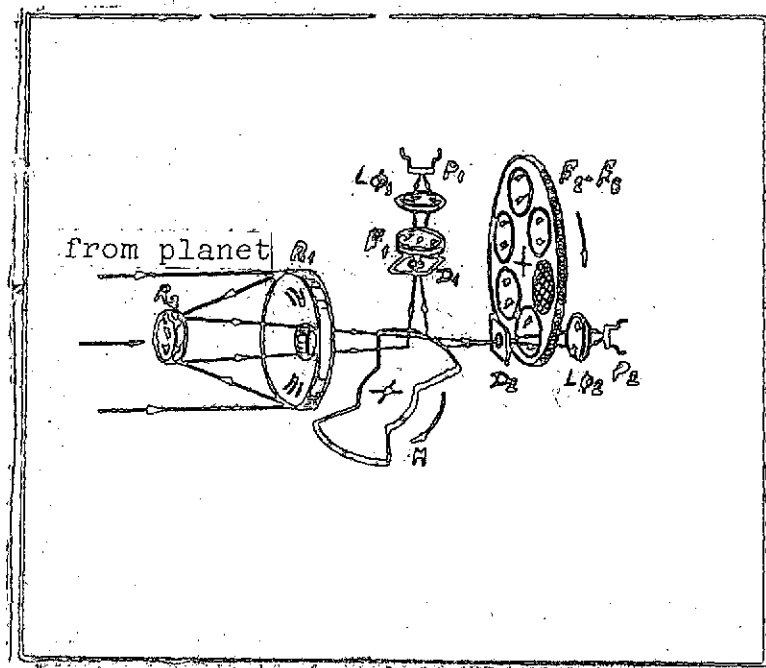


Fig. 2. Optical diagram of CO₂ photometer.

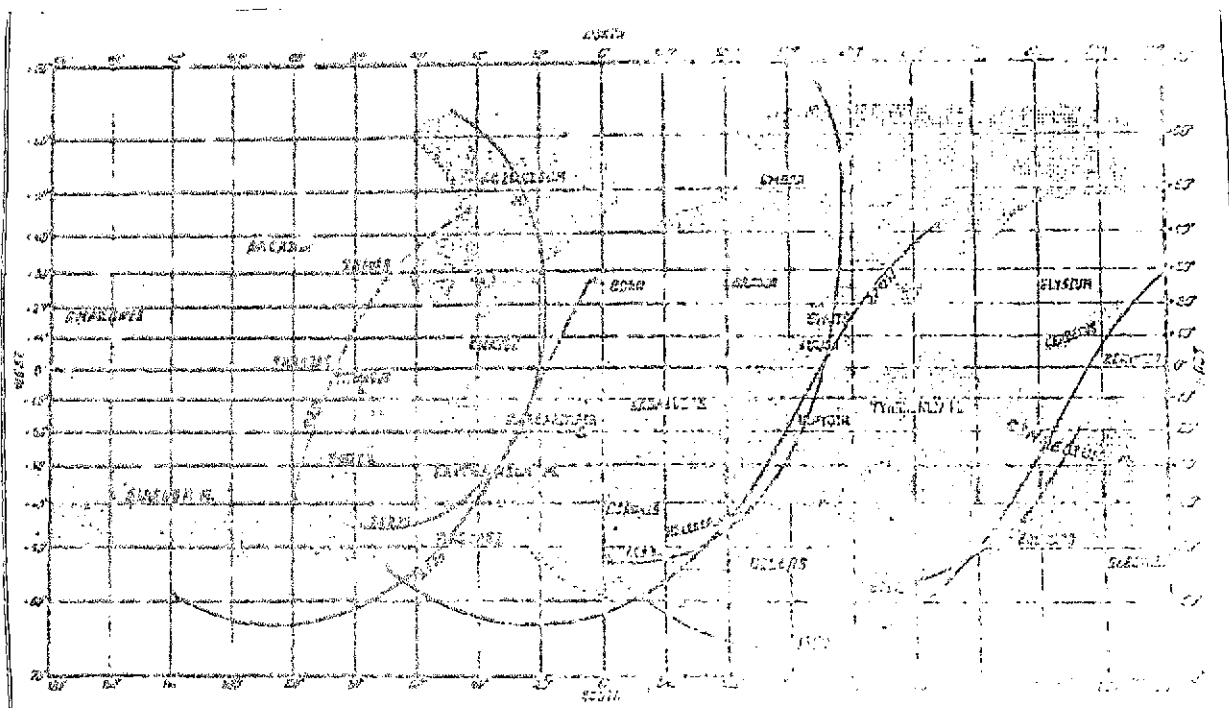


Fig. 3. Measurement courses of Mars-3 astrophysical instrument set.

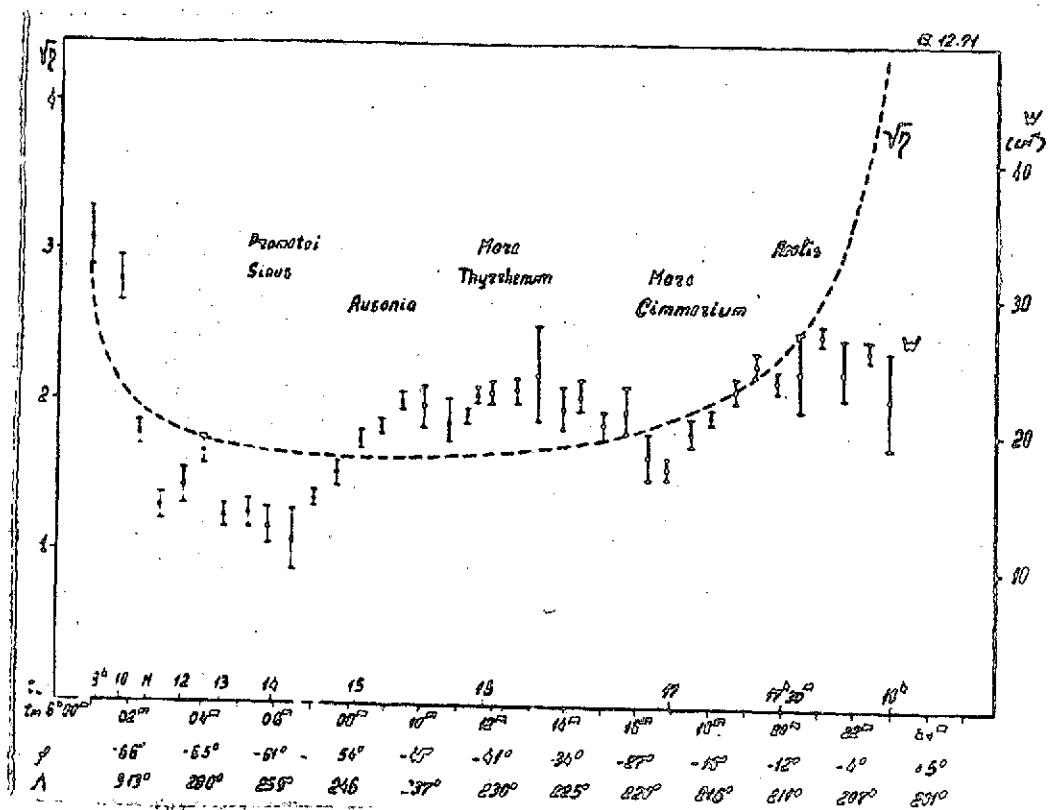


Fig. 4. Equivalent widths of $\lambda = 2.05 \mu\text{m}$ CO_2 band on 15 December 1971 measurement course (curve W). η is air mass. Moscow time t_M , local time t_L , latitude ϕ and longitude λ on abscissa.

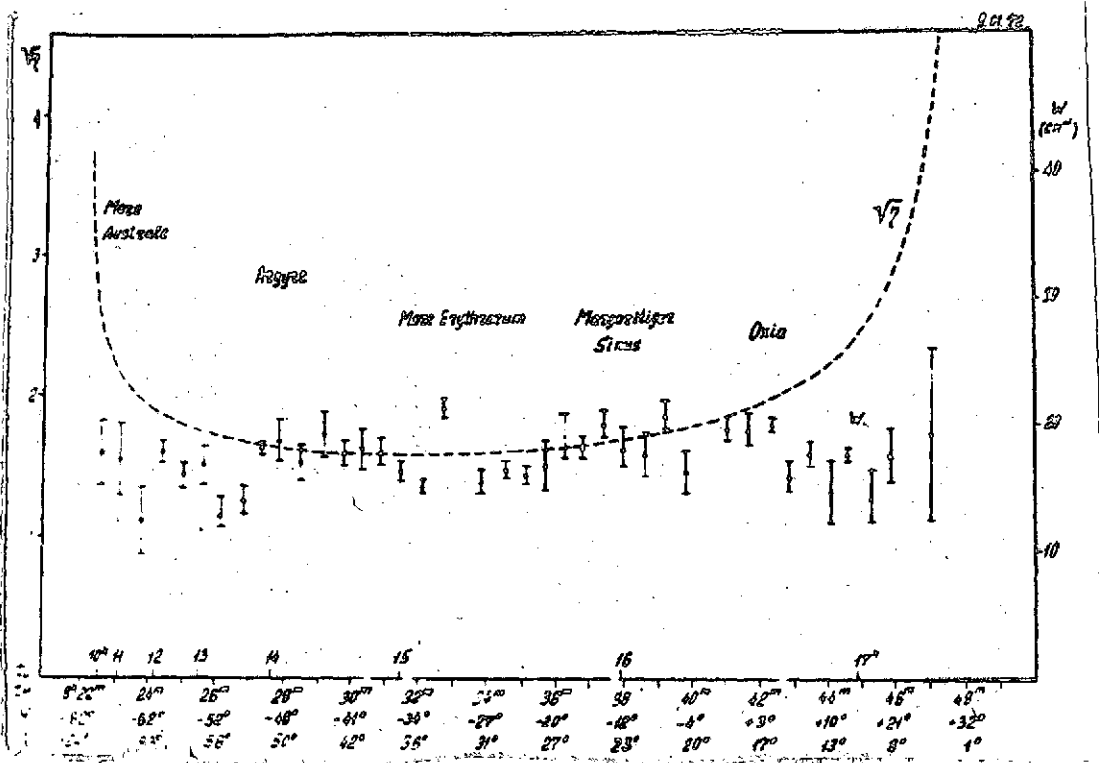


Fig. 6. Same as in Fig. 4 from 9 January 1972 measurements.

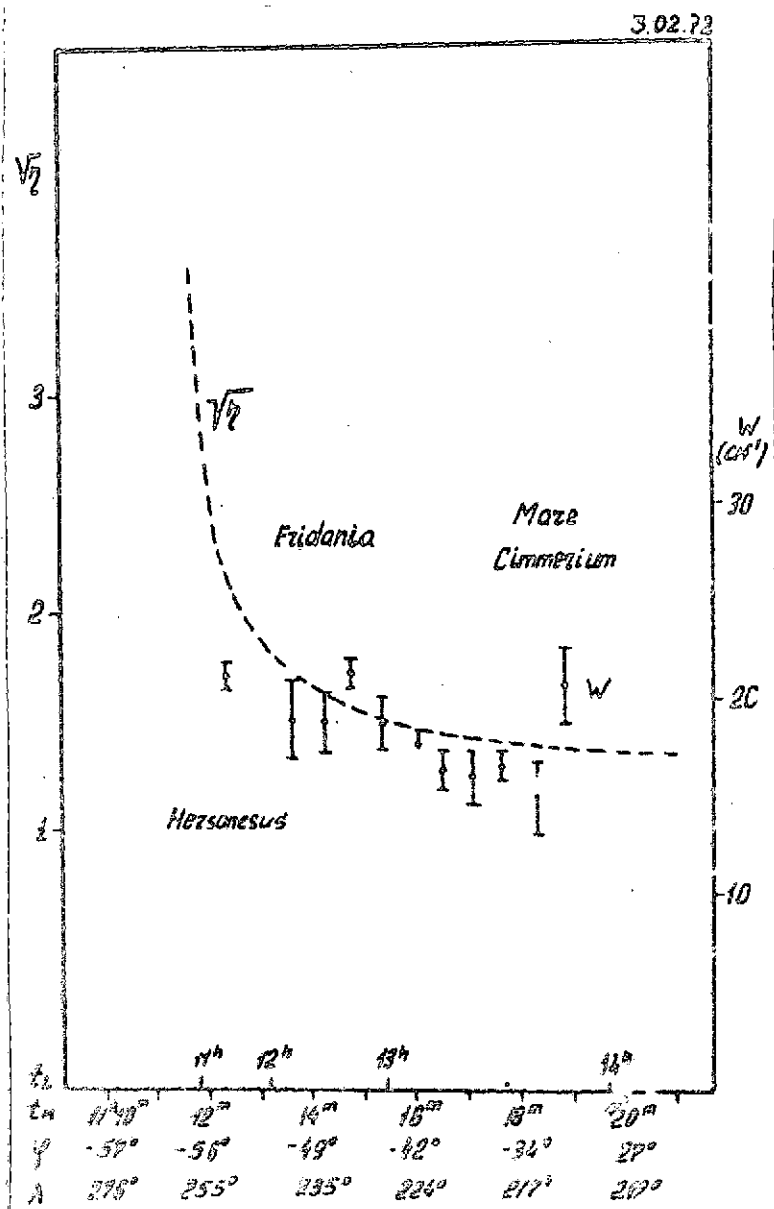


Fig. 7. Same as in Fig. 4 from
3 February 1972 measurements.

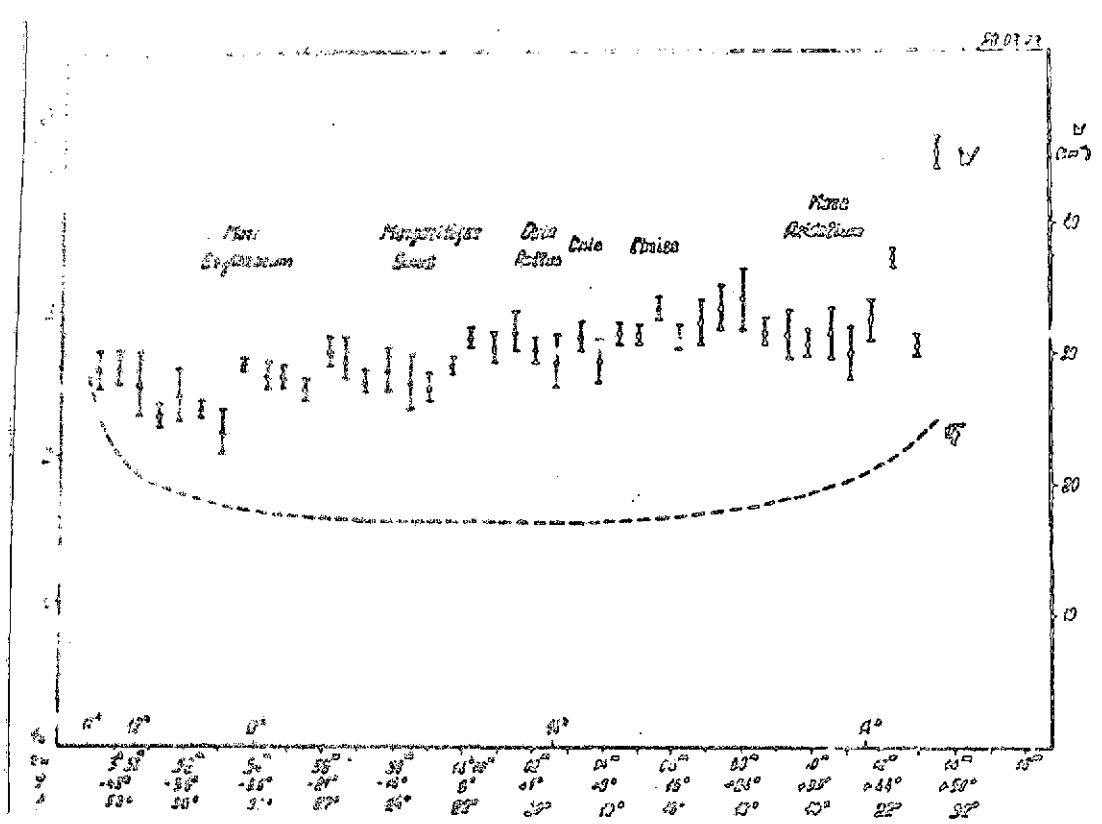


Fig. 9. Same as in Fig. 4 from 28 February 1972 measurements.

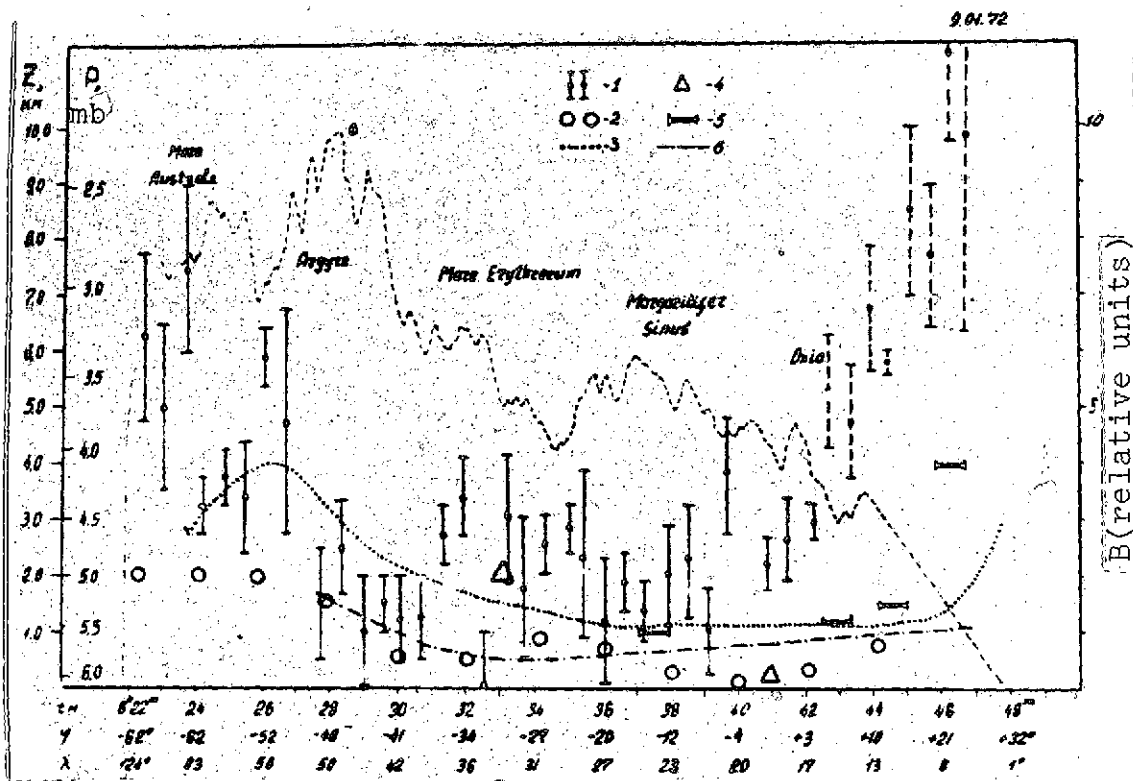


Fig. 10. Altitudes Z and pressures P from measurements on 9 January 1972 course. Moscow time t_M , latitude ϕ and longitude λ on abscissa. 1. Mars-3, 2. Mariner-9 (IR), 3. ground CO_2 measurements, 4. Mariner-9 (radio occultation), 5. ground-based radar, 6. Mariner-9 (UV).

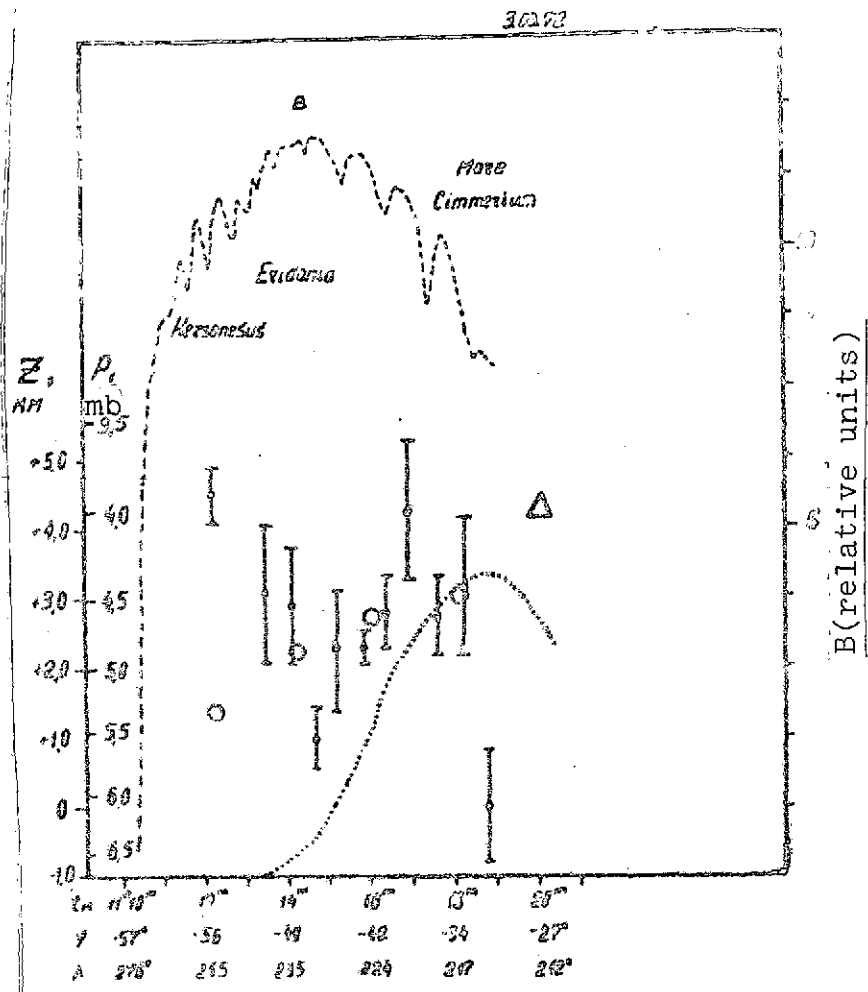


Fig. 11. Same as in Fig. 10 from 3 February 1972 measurements.

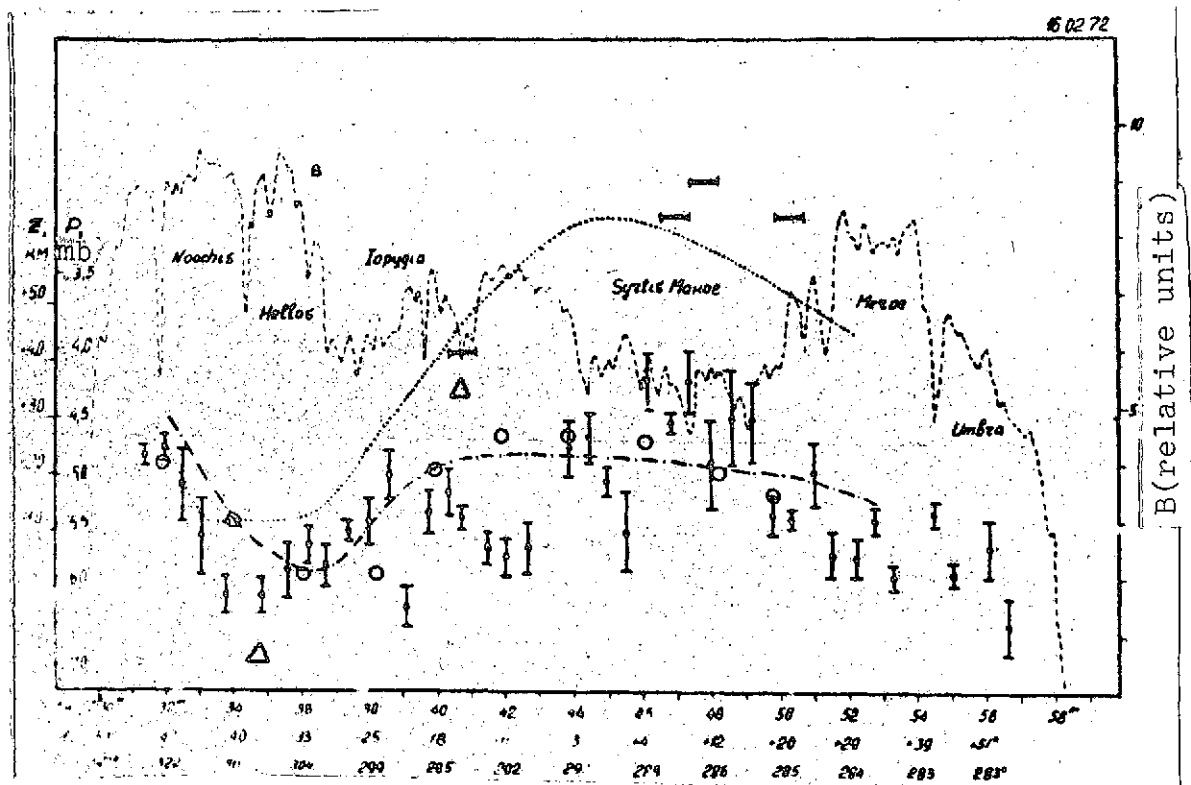


Fig. 12. Same as in Fig. 10 from 16 February 1972 measurements.

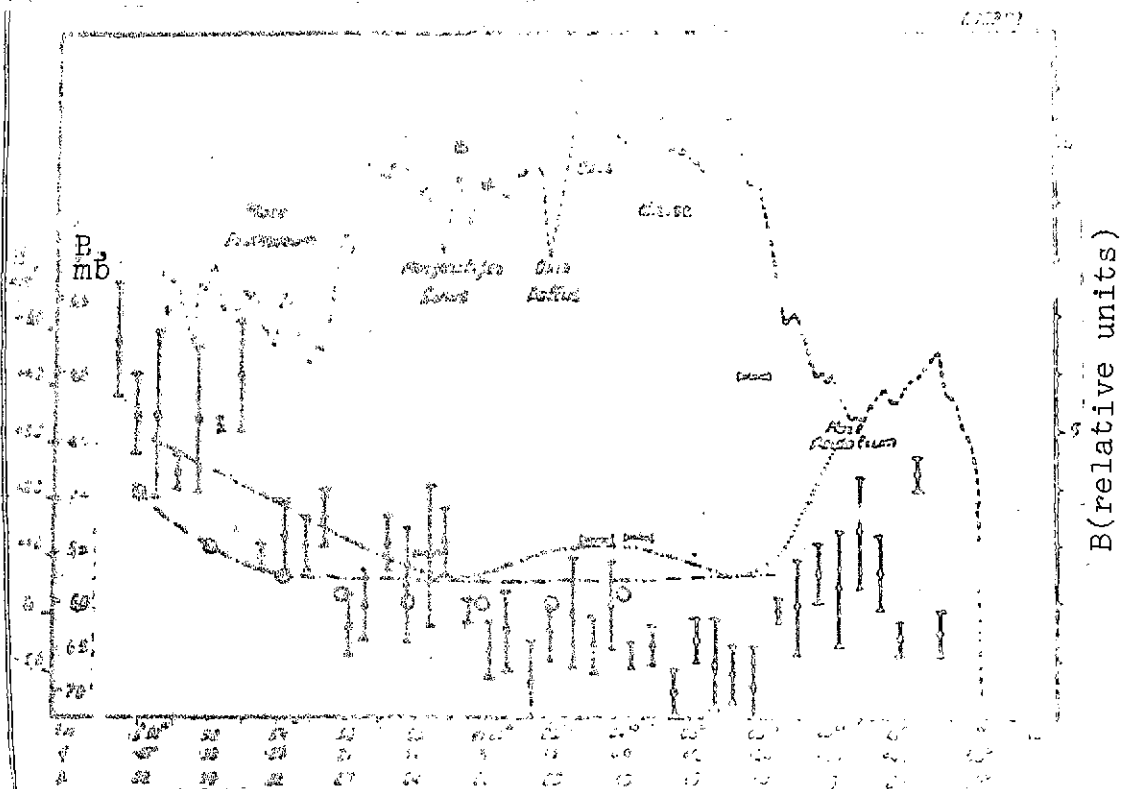


Fig. 13. Same as in Fig. 10 from 28 February 1972 measurements.

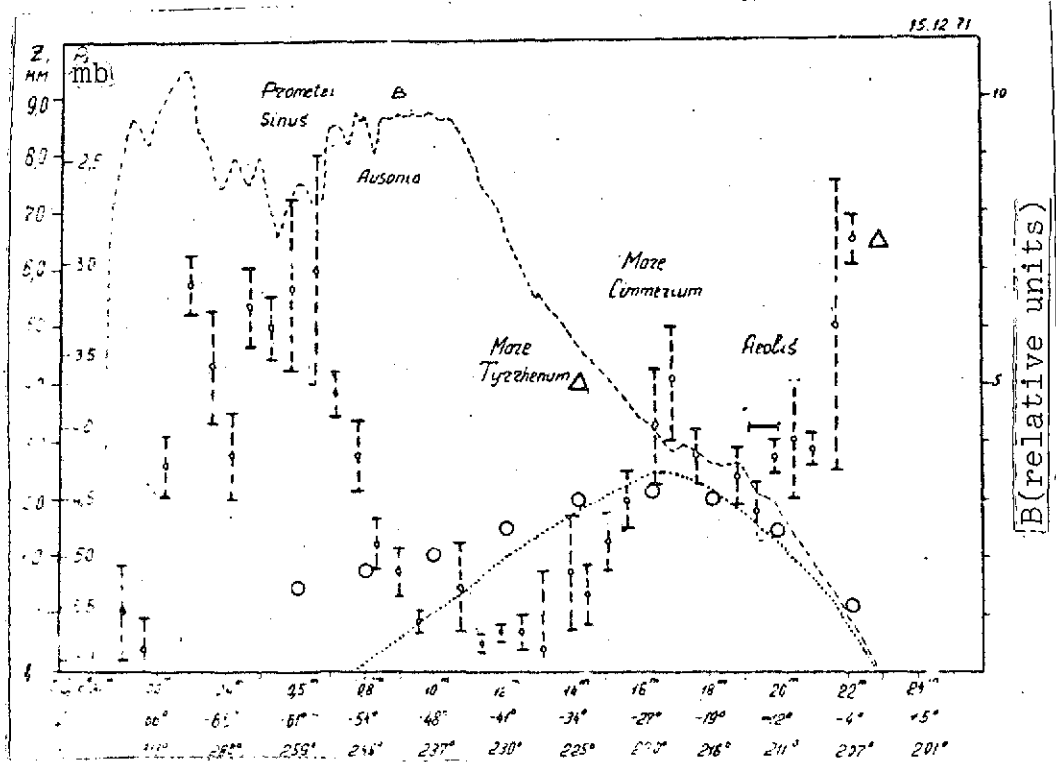


Fig. 14. Same as in Fig. 10 from 15 December 1971 measurements (dust storm still not ended, Mars-3 CO₂ altimetry data unreliable).

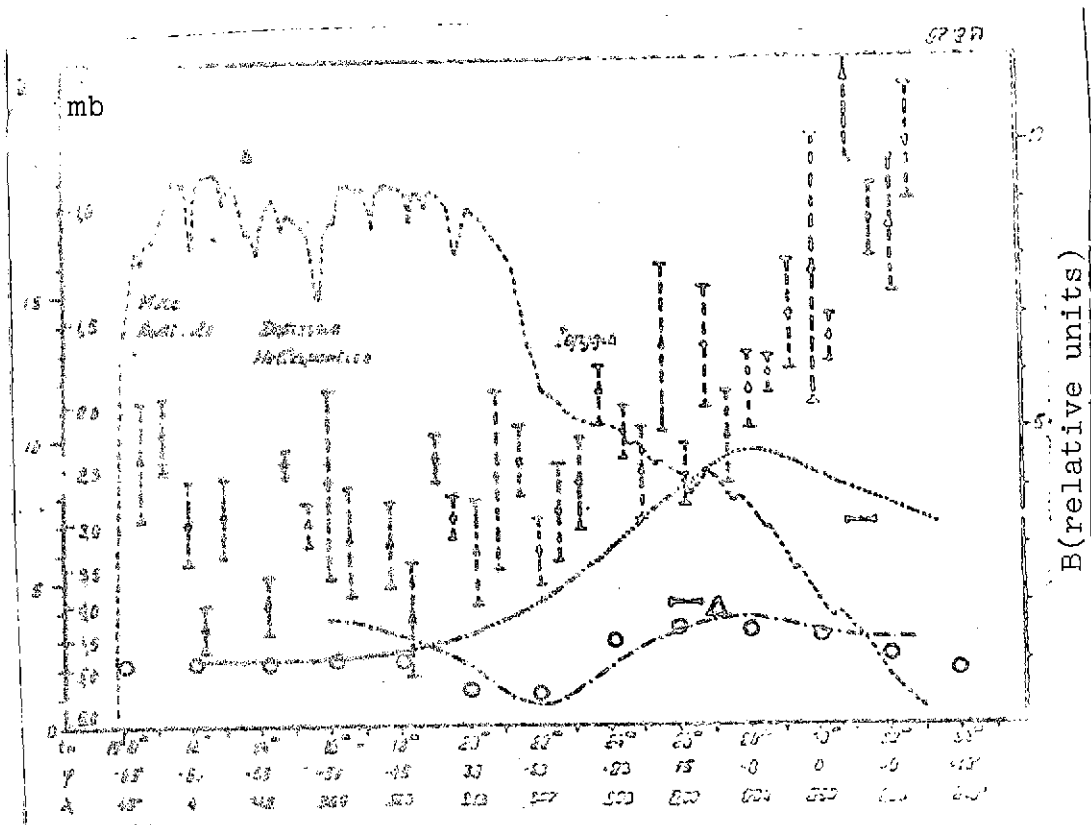


Fig. 15. Same as in Fig. 10 from 27 December 1971 measurements (dust storm still not ended, Mars-3 CO₂ altimetry data unreliable).

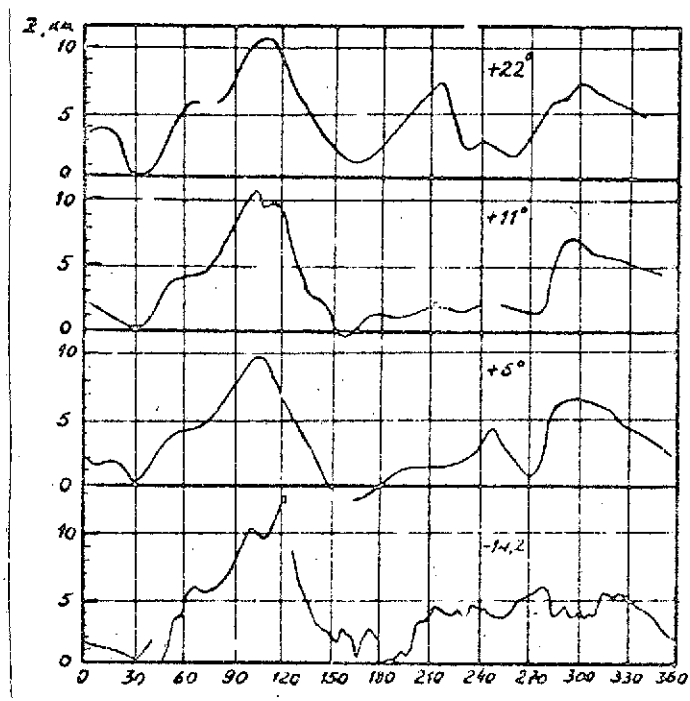


Fig. 16. Altitude profiles obtained as a result of ground-based radar at 3.8 cm in 1967 [1], 1969 [2], and 1971 [4]. 1971 profile somewhat smoothed. Level at longitude 30° is provisionally adopted as zero in all cross sections.

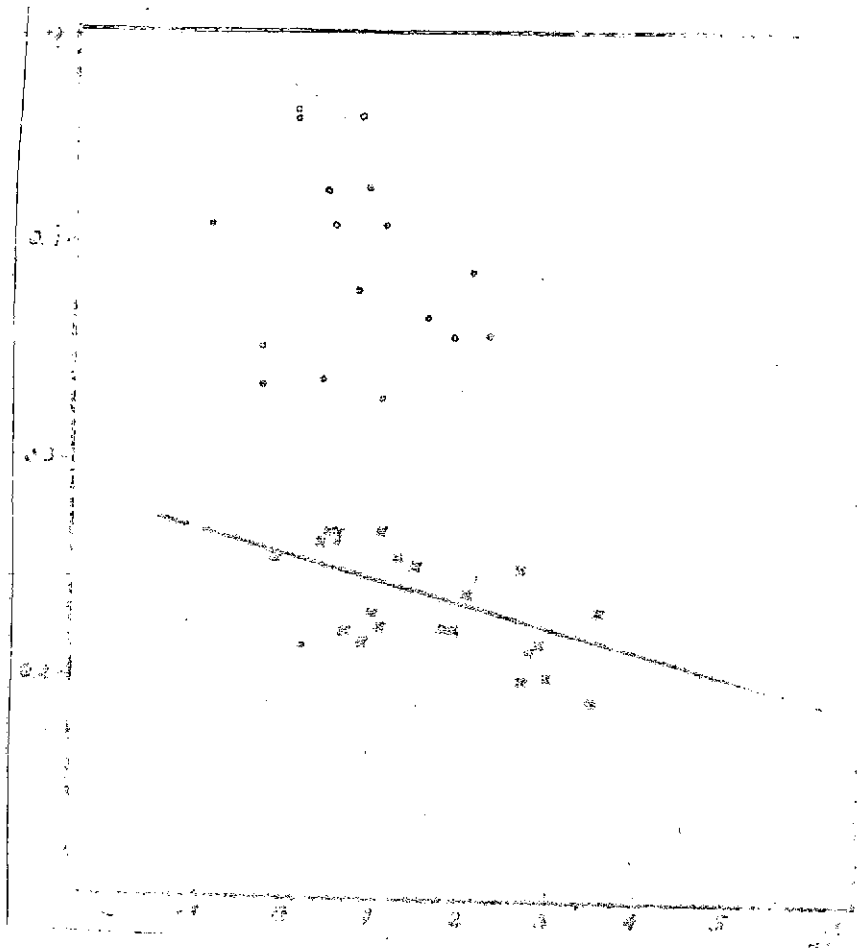


Fig. 17. Correlation between altitudes and brightness factors on 16 February course. Altitudes on abscissa, relative brightness factors on ordinate. Lower group of points concern band of dark regions, upper group, light regions in southern and northern parts of course. Points used in calculation of statistical R vs. Z are marked by crosses (see Table 1).

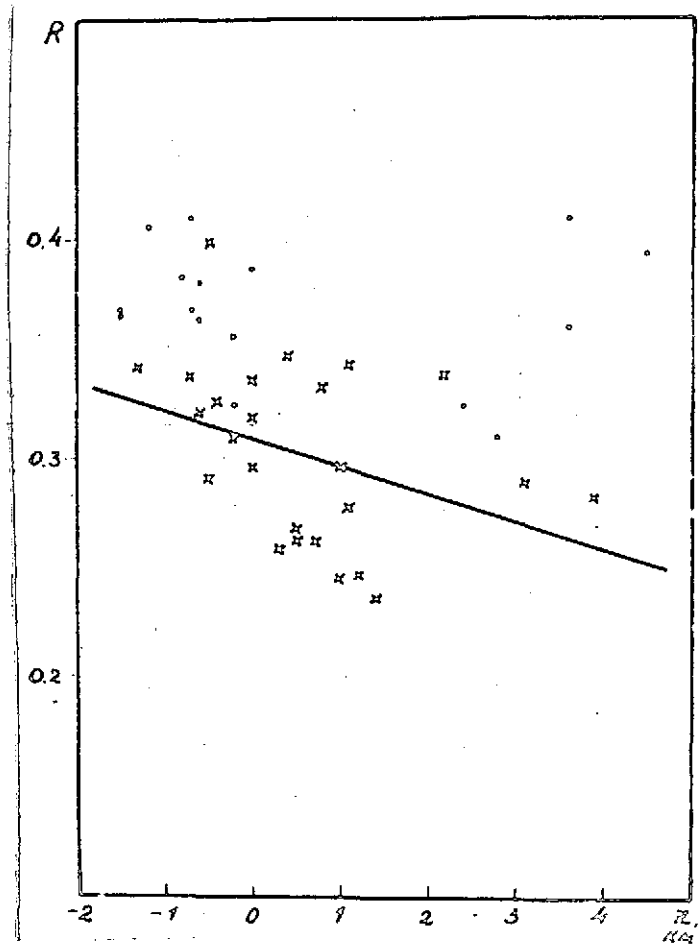


Fig. 18. Same as in Fig. 17 for 28 February course. Three points on the upper right concern the southern section of the course.

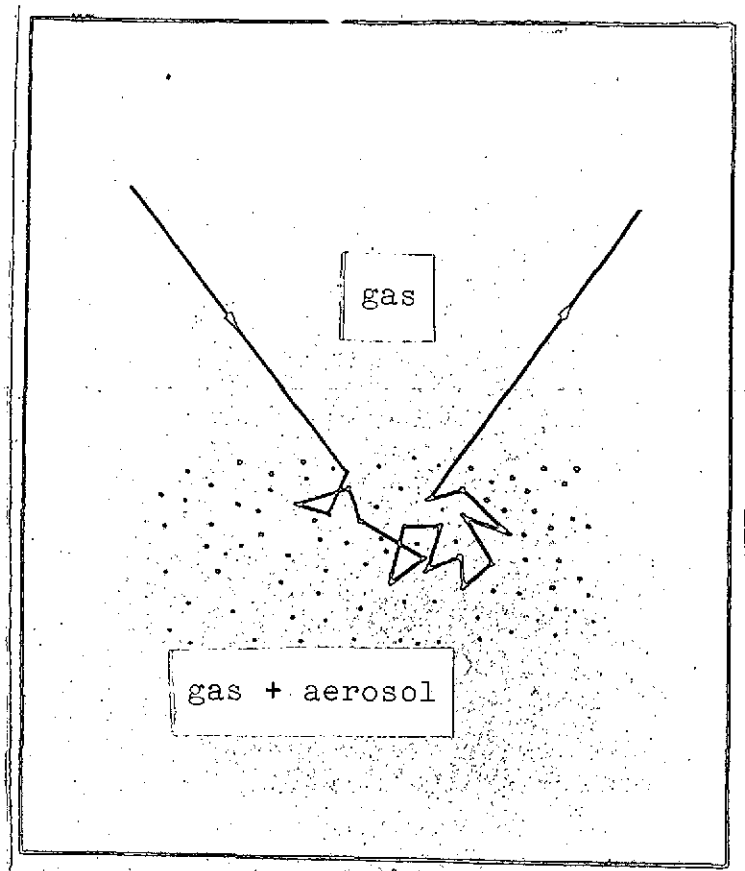


Fig. 19. Schematic illustration of geometry of propagation of radiation in scattering medium.